Preprints of the 19th World Congress
The International Federation of Automatic Control
Cape Town, South Africa. August 24-29, 2014

Unmanned Aerial Vehicles Model Identification using Multi-Objective Optimization Techniques

J. Velasco, S. García-Nieto.

Instituto Universitario de Automática e Informática Industrial. Universitat Politècnica de València, 46022 Valencia Spain (e-mail: jevecar@upvnet.upv.es)

Abstract: The total amount of UAVs civil applications is getting bigger and bigger. The cost and the risks of the development phase of this systems has to be decreased in order to make them affordable. It is required to minimize the number of hours of real flight, making use of simulation tools and taking full advantage of the acquired data. Thus, obtaining a dynamic model that tightly adjusts to the real flight behaviour of the aircraft gains in importance, in the way that it will lead to precise simulation results and, therefore, to correctly designed control algorithms. A model identification technique based on experimental data and Multi-Objective optimization evolution algorithm, is presented here. This methodology makes profit of the possibility given by this type of algorithm of facing different objetives at the same time, to take full advantage of the experimental data and to get better adjusted models.

Keywords: Automated guided vehicles, Multiobjective optimizations, Identification, Least-squares method.

1. INTRODUCTION

There exists an increasingly popular variety of applications that justify the development of Unmanned Aerial Vehicles (UAVs) in the civil aviation field. Tasks such as photography for coastline control and beaches erosion tracing, fire detection and control (Krüll et al., 2012), infrastructures inspection, or measurement for agriculture (Xiang and Tian, 2011) are just some of the possible applications. In this new aeronautics field, a sufficiently low cost, which suits companies requierments is the main objective.

There are several fronts that have to be attended for the achievement of this aim. First, it is necessary to reduce the cost of the aircraft itself. This brings therefore, a completely new generation of tiny airplanes, which size is the minimum necessary to house propulsion, sensorization and control equipments.

Second, the integrated systems (sensors, actuators and control units), have to be powerful enough to control the fast dynamics of these vehicles and carry out, at the same time, the mission for which they have been purchased. The cost of such devices is becoming lower and lower, thanks to the fast evolution experienced by the computer technology in the last few years.

Finally, because of the characteristics of the product, the cost of the development phase has become an important percentage of the final price. It is required in this point to minimize the number of hours of real flight, making use of simulation tools and squeezing, as much as possible, already acquired data. Besides, it is in this phase in which the hardware integrity is in bigger danger. Thus, obtaining a dynamic model that tightly adjusts to the real flight behaviour of the aircraft seems vital, in the way that it will lead to precise simulation results and, therefore, to correctly designed control algorithms.

In this article, a methodology based on Multi-Objective (MO) optimization is presented and applied to a real system. To present this methodolgy, flight data are used instead of wind tunnel experiments, to identify the non-dimensional derivatives of stability and control of an UAV. Nevertheless, the technique exposed is not limited by the data source, but the other way around, it is enhanced with the quality and diversity of the performed experiments. As an example of this, despite experiments in this article are lacking measures relative to air, once available, they could be added in a straightforward manner to the identification process, with the obvious improvement of the obtained results, but without any change on the methodology itself. Thus, the presented identification technique allows the designer to test flight data from different types of experiment and, thereby, to obtain models with acceptable performances in several kinds of situation.

The article is devided in 5 sections. Section 2 introduces the aircraft and the hardware used in the experiments, along with the dynamic and aerodynamic models willing to be identified. In section 3 the methodology used in the identification will be shown and explained. Flight tests are presented in section 4. Every experiment has been performed twice so that a second set of values could be obtained for validating results. Results from the identification and the validation processes are also given

⋆ This work has been partially funded by the Government of Spain through the project TIN2011-28082 and by the UPV through the project PAID-06-11.

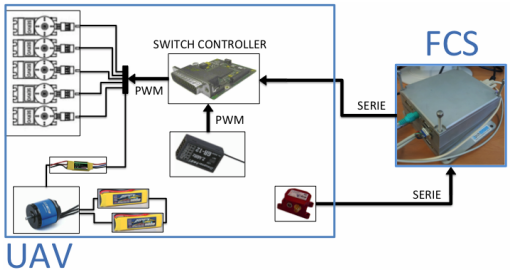

Fig. 1. Interconnection between UAV devices and FCS

in section 4. Finally, some conclusions are commented in section 5.

2. UAV TESTBENCH

2.1 Platform and Hardware

As the main component of the flight platform, a Kadett 2400 aircraft, manufactured by Graupner, may be found. It houses all necessary devices for its control, not only manually, but also in autonomous mode. During normal flight, 3 control surfaces are provided: tail rudder, elevators and ailerons. As the unit of propulsion a brushless engine of altern current is integrated, which is fed by two LIPO batteries through a frequency variator. Alike the servomotors, the variator is controlled by sending PWM signals as commanding signals.

There exists a device bridge between the manual and the autonomous states. The SSC (Servo Switch Controller) is able to perform the commutation between different sources of entrance. However, its principle property is allowing a computer to measure and also to introduce deflections in control surfaces (δ) and changes in the motor thrust (T).

As already stated, control actions are sent from the Flight Control Station (FCS), constituted by a PC-104. Is this unit the one housing the control algorithms, performing, therefore, all necessary tasks at each phase of the flight. The loop is closed by the IG500N unit. This all-in-one device, joins the efforts of a wide range of sensors, such as accelerometers, giroscopes and magnetometers. Its Kalman filter is capable of mixing the information comming from those sensors in order to offer precise mesurements of position, orientation, linear and angular speed, and acceleration, in the 3 aircraft body-axes. This same platform was presented in (Velasco et al. (2012), Velasco et al. (2013) and Velasco (2013)) together with the results of the first flight tests. The figure 1 shows the hardware elements described here.

2.2 Aircraft Dynamic Model

Once the hardware platform has been introduced, a model that approximately explains the behaviour of the real process is going to be derived. In this case, the final model will be used for simulation and design of control algorithms for a UAV. This means obtaining the expressions that relate the input variables: deflection in the control surfaces and motor load; to a series of output signals: linear and angular velocities, accelerations and position in 3D space.

As expressed in (Klein and Morelli, 2006), the seeking of these expressions normally begins from the linear and the angular momentum conservation principles, that can be expressed as:

$$\sum_{ext} \overrightarrow{F} = \frac{d}{dt}(m\overrightarrow{V}) \tag{1}$$

$$\sum_{ext} \overrightarrow{M} = \frac{d}{dt}(I\overrightarrow{\omega}) \tag{2}$$

Where $\sum_{ext} \overrightarrow{F}$ and $\sum_{ext} \overrightarrow{M}$ are the summ of external forces and moments respectively, m and I are the mass and the inertia tensor of the aircraft, and $\overrightarrow{V}$ and $\overrightarrow{\omega}$ are linear and angular velocity vectors. In particular 3 are the types of external forces that affect to the behaviour of the vehicle. They are: aerodynamic force (F_A), force applied by the motor (F_T) and the gravitational force (F_G). At the same time, only the aerodynamic force generates aerodynamic torque (M_A). Thereby, the equations 1 and 2 remain:

$$\overrightarrow{F_A} + \overrightarrow{F_T} + \overrightarrow{F_G} = m\dot{\overrightarrow{V}} + \overrightarrow{\omega} \times \overrightarrow{V} \tag{3}$$

$$\overrightarrow{M_A} = I\dot{\overrightarrow{\omega}} + \overrightarrow{\omega} \times I\overrightarrow{\omega} \tag{4}$$

The two previous equations are actually vectorial equations, so that, there is a total of 6 equations that correspond to the 6 degrees of freedom of a rigid body in the space. Deriving 3 and 4 the following expressions are obtained:

$$\begin{aligned} \bar{q}S\begin{bmatrix} C_X \\ C_Y \\ C_Z \end{bmatrix} + \begin{bmatrix} -g\sin\theta \\ g\sin\phi\cos\theta \\ g\cos\phi\cos\theta \end{bmatrix} + \begin{bmatrix} T \\ 0 \\ 0 \end{bmatrix} \\ = m\begin{bmatrix} \dot{u} \\ \dot{v} \\ \dot{w} \end{bmatrix} + \begin{bmatrix} p \\ q \\ r \end{bmatrix} \times m\begin{bmatrix} u \\ v \\ w \end{bmatrix} \end{aligned} \tag{5}$$

$$\begin{aligned} \bar{q}S\begin{bmatrix} bC_l \\ \bar{c}C_m \\ bC_n \end{bmatrix} = \begin{bmatrix} I_x & 0 & -I_{xz} \\ 0 & I_y & 0 \\ -I_{zx} & 0 & I_z \end{bmatrix}\begin{bmatrix} \dot{p} \\ \dot{q} \\ \dot{r} \end{bmatrix} \\ + \begin{bmatrix} p \\ q \\ r \end{bmatrix} \times \begin{bmatrix} I_x & 0 & -I_{xz} \\ 0 & I_y & 0 \\ -I_{zx} & 0 & I_z \end{bmatrix}\begin{bmatrix} p \\ q \\ r \end{bmatrix} \end{aligned} \tag{6}$$

Where u, v, and w are the components of the linear velocity of the aircraft in its body axes (x_b, y_b, z_b). In the same way, p, q, and r are the 3 componentes of the angular velocity. It is important to highlight the apparition in the equations 5 and 6 of the variables C_i, that represent the aerodynamic coefficients of each component of the resultant aerodynamic force (X, Y, and Z) and torque (L, N, and M). Such coefficients, are functions that relate those components to some of the system variables. The expressions that those coefficients adopt is of great interest in this work and therefore, they will be studied in further detail in section 2.3. Finally S, b, $\bar{c}$ are constructive constants of the aeroplane and $\bar{q}$ is the dynamic pressure of the air.

The aircraft orientation is usually denoted with the well known Euler angles of roll ϕ, pitch θ, and yaw ψ, wich express the rotation of a body from a global reference system to the body-axes. The kinematic equations that

relate angular velocities of the aircraft to the Euler angles are:

$$\begin{bmatrix} p \\ q \\ r \end{bmatrix} = \begin{bmatrix} 1 & 0 & -\sin\theta \\ 0 & \cos\theta & \sin\phi\cos\theta \\ 0 & -\sin\phi & \cos\phi\cos\theta \end{bmatrix} \begin{bmatrix} \dot{\phi} \\ \dot{\theta} \\ \dot{\psi} \end{bmatrix} \tag{7}$$

Finally, equations 8 to 16 are the result of reordering equations 5, 6, and 7, so that they can be directly used on the calculation of the simulation output values. Such values will be the same as those coming from the unit IG500N in real flights.

Force equations:

$$\dot{u} = rv - qw + \frac{\overline{q}S}{m}C_X(\delta) - g\sin\theta + \frac{T}{m} \tag{8}$$

$$\dot{v} = pw - ru + \frac{\overline{q}S}{m}C_Y(\delta) + g\cos\theta\sin\phi \tag{9}$$

$$\dot{w} = qu - pv + \frac{\overline{q}S}{m}C_Z(\delta) + g\cos\theta\cos\phi \tag{10}$$

Torque equations:

$$\dot{p} - \frac{I_{xz}}{I_x}\dot{r} = \frac{\overline{q}Sb}{I_x}C_l(\delta) - \frac{I_z - I_y}{I_x}qr + \frac{I_{xz}}{I_x}qp \tag{11}$$

$$\dot{q} = \frac{\overline{q}S\overline{c}}{I_y}C_m(\delta) - \frac{I_x - Iz}{I_y}pr - \frac{I_{xz}}{I_y}(p^2 - r^2) \tag{12}$$

$$\dot{r} - \frac{I_{xz}}{I_z}\dot{p} = \frac{\overline{q}Sb}{I_z}C_n(\delta) - \frac{I_y - I_x}{I_z}pq - \frac{I_{xz}}{I_z}qr \tag{13}$$

Kinematic equations:

$$\dot{\phi} = p + \tan\theta(q\sin\phi + r\cos\phi) \tag{14}$$

$$\dot{\theta} = q\cos\phi - r\sin\phi \tag{15}$$

$$\dot{\psi} = \frac{q\sin\phi + r\cos\phi}{\cos\theta} \tag{16}$$

2.3 Aircraft Aerodynamic Model

It was said in 2.2 that aerodynamic forces and torques were related to some of the system variables through a series of functions that were called aerodynamic coefficients. In this section the structure used in the present article for those functions will be stated and, likewise, the parameters to be identified will be highlighted.

In (Klein and Morelli, 2006) detailed information on how to proceed to obtain the dependencies of aerodynamic coefficients with other system variables is provided. First, if we assume a scenario in which the aircraft is generally in steady flight conditions, and it only performs short maneuvers that take it off from this state, we can truncate the Taylor series expansion to keep only the first or second order terms. Furthermore, under this assumption of small perturbations, and based on the symmetry of the vehicle, it can be assumed that 1) the symmetrical (longitudinal) variables u, w and q do not affect asymmetrical (lateral) force and torques Y, L and N; and similarly, 2) asymmetric (lateral) variables v, p and r do not affect the symmetrical (longitudinal) forces and torque X, Z and M.

Equations from (17) to (22) show the approximation of the aerodynamic equations that have been adopted for this article.

Longitudinal aerodynamic models:

$$\begin{aligned} C_D(t) =& \mathbf{C_{D_0}} + \mathbf{C_{D_V}}\frac{1}{V_0}\Delta V(t) + \mathbf{C_{D_\alpha}}\Delta\alpha(t) \\ &+ \mathbf{C_{D_{\alpha^2}}}\Delta\alpha(t)^2 + \mathbf{C_{D_q}}\frac{\overline{c}}{2V_0}q(t) + \mathbf{C_{D_{\delta_e}}}\Delta\delta_e(t) \end{aligned} \tag{17}$$

$$\begin{aligned} C_L(t) =& \mathbf{C_{L_0}} + \mathbf{C_{L_V}}\frac{1}{V_0}\Delta V(t) + \mathbf{C_{L_\alpha}}\Delta\alpha(t) \\ &+ \mathbf{C_{L_{\alpha^2}}}\Delta\alpha(t)^2 + \mathbf{C_{L_{\dot{\alpha}}}}\frac{\overline{c}}{2V_0}\dot{\alpha}(t) + \mathbf{C_{L_q}}\frac{\overline{c}}{2V_0}q(t) \\ &+ \mathbf{C_{L_{\delta_e}}}\Delta\delta_e(t) \end{aligned} \tag{18}$$

$$\begin{aligned} C_m(t) =& \mathbf{C_{m_0}} + \mathbf{C_{m_V}}\frac{1}{V_0}\Delta V(t) + \mathbf{C_{m_\alpha}}\Delta\alpha(t) \\ &+ \mathbf{C_{m_{\alpha^2}}}\Delta\alpha(t)^2 + \mathbf{C_{m_{\dot{\alpha}}}}\frac{\overline{c}}{2V_0}\dot{\alpha}(t) \\ &+ \mathbf{C_{m_q}}\frac{\overline{c}}{2V_0}q(t) + \mathbf{C_{m_{\delta_e}}}\Delta\delta_e(t) \end{aligned} \tag{19}$$

Lateral aerodynamic models:

$$\begin{aligned} C_Y(t) =& \mathbf{C_{Y_0}} + \mathbf{C_{Y_\beta}}\Delta\beta(t) + \mathbf{C_{Y_p}}\frac{b}{2V_0}p(t) \\ &+ \mathbf{C_{Y_r}}\frac{b}{2V_0}r(t) + \mathbf{C_{Y_{\delta_{al}}}}\Delta\delta_{al}(t) + \mathbf{C_{Y_{\delta_r}}}\Delta\delta_r(t) \end{aligned} \tag{20}$$

$$\begin{aligned} C_l(t) =& \mathbf{C_{l_0}} + \mathbf{C_{l_\beta}}\Delta\beta(t) + \mathbf{C_{l_p}}\frac{b}{2V_0}p(t) \\ &+ \mathbf{C_{l_r}}\frac{b}{2V_0}r(t) + \mathbf{C_{l_{\delta_{al}}}}\Delta\delta_{al}(t) + \mathbf{C_{l_{\delta_r}}}\Delta\delta_r(t) \end{aligned} \tag{21}$$

$$\begin{aligned} C_n(t) =& \mathbf{C_{n_0}} + \mathbf{C_{n_\beta}}\Delta\beta(t) + \mathbf{C_{n_p}}\frac{b}{2V_0}p(t) \\ &+ \mathbf{C_{n_r}}\frac{b}{2V_0}r(t) + \mathbf{C_{n_{\delta_{al}}}}\Delta\delta_{al}(t) + \mathbf{C_{n_{\delta_r}}}\Delta\delta_r(t) \end{aligned} \tag{22}$$

Where α and β are the angle of attack and of sideslip respectively and V is the airspeed. In particular, V_0 is the airspeed measured at the steady state of flight, before a maneuver begins. Theese variables are velocity dependent and they can be calculated as follows:

$$\alpha = \arctan\left(\frac{w}{u}\right) \quad ; \quad \beta = \arcsin\left(\frac{v}{V}\right) \tag{23}$$

$$V = |\overrightarrow{V}| = \sqrt{u^2 + v^2 + w^2} \tag{24}$$

Besides, C_L and C_D are the Lift and Drag coefficients and their relation with C_X and C_Z is:

$$C_L(t) = -C_Z(t)\cos(\alpha(t)) + C_X(t)\sin(\alpha(t)) \tag{25}$$

$$C_D(t) = -C_X(t)\cos(\alpha(t)) - C_Z(t)\sin(\alpha(t)) \tag{26}$$

Thus, the aerodynamic model identification is based on extracting the polynomial constants of the equations 17 to 22 (marked in bold) from the flight data and by means of the dynamic model. Those constants are called non-dimmensional derivatives of stability and control.

3. AERODYNAMIC MODEL IDENTIFICATION

3.1 Previous calculations

It is easy to understand that there is no sensor capable of measuring aerodynamic coefficients directly. Thus, before

performing the optimization it is necessary to calculate the actual value of the aerodynamic coefficients during the flight. The dynamic model equations will be used for that purpose.

Equations 27 to 32 describe the methodology used to obtain the values taken by the aerodynamic coefficients at the time instants in which measurements are available. These equations are easily deduced from the first principles model presented in 2.2 (Klein and Morelli, 2006).

$$C_X(t) = \frac{1}{\overline{q}(t)S}(ma_x(t) - T(t)) \tag{27}$$

$$C_Y(t) = \frac{ma_y(t)}{\overline{q}(t)S} \tag{28}$$

$$C_Z(t) = \frac{ma_z(t)}{\overline{q}(t)S} \tag{29}$$

$$C_l(t) = \frac{1}{\overline{q}(t)Sb}\begin{array}{l}[I_x\dot{p}(t) - I_{xz}\left(p(t)q(t) + \dot{r}(t)\right) \\ + \left(I_z - I_y\right)q(t)r(t)]\end{array} \tag{30}$$

$$C_m(t) = \frac{1}{\overline{q}(t)S\overline{c}}\begin{array}{l}[I_y\dot{q}(t) + \left(I_x - I_z\right)p(t)r(t) \\ + I_{xz}\left(p(t)^2 - r(t)^2\right)]\end{array} \tag{31}$$

$$C_n(t) = \frac{1}{\overline{q}(t)Sb}\begin{array}{l}[I_z\dot{r}(t) - I_{xz}\left(\dot{p}(t) - q(t)r(t)\right) \\ + \left(I_y - I_x\right)p(t)q(t)]\end{array} \tag{32}$$

Refer to equations 25 and 26 for the calculation of $C_L(t)$ and $C_D(t)$ respectevely.

3.2 Multi-Objective Optimization

In engineering problems, it is a common issue to deal with situations that require the optimization of multiple objectives that include, in addition, physical constraints, operational constraints and nonlinearities. Due to this fact, addressing these problems from the standpoint of classical optimization could be insufficient.

Any multiobjective optimization problem (MOP) can be stated as:

$$\min_{\theta\in\mathbb{R}} J(\theta) = [J_1(\theta), J_2(\theta), \ldots, J_m(\theta)] \tag{33}$$

Where θ is the solution that minimazes the m cost functions J_i at the same time. Generally, it will not be possible to find a solution that satisfies all requirements at the same time, so the optimizer will have to provide the amount of solutions which are not improved by any other in all the objectives at the same time. That set of solutions is the Pareto set and their value in the objectives space is the Pareto front.

Multiobjective techniques applied to model identification have achieved great results in many cases, as shown in (Rodriguez-Vazquez and Fleming (1998), Herrero et al. (2007) and Yousefi et al. (2008)).

In our case, elevators deflection and motor thrust variations, generate changes in longitudinal variables and, in the same way, ailerons and rudder deflections do likewise in lateral ones. Therefore, longitudinal and lateral coefficient models can be identified from different kind of experiments. As an example, if a C_D modeled is obtained by optimizing an elevators test, the model performance on a motor experiment data will be deacreased, and viceversa. Therefore, an identification that takes both experiments in account at the same time, may be stated as a biobjective optimization problem.

If the Mean Square Error (MSE) is used as performance index of the identification process, two cost functions can be defined for each aerodynamic coefficient. Equations 34 and 35 are the two cost functions to minimize for obtaining any of the longitudinal models.

$$J_1 = \frac{1}{N_{elevator}}\sum_{i=1}^{N_{elevator}}\left(C_j(t_i) - \hat{C}_j(t_i)\right)^2 \quad \forall j \in \{D, L, m\} \tag{34}$$

$$J_2 = \frac{1}{N_{motor}}\sum_{i=1}^{N_{motor}}\left(C_j(t_i) - \hat{C}_j(t_i)\right)^2 \quad \forall j \in \{D, L, m\} \tag{35}$$

where $\hat{C}_j(t_i)$ is the model approximation of the C_j value at the instant t_i and $N_{elevator}$ and N_{motor} are the number of samples of each kind of experiment. Similar cost functions can be defined for the three lateral models.

Then, if, $C_l(t)$ is to be modeled by using one ailerons experiment and one rudder experiment, the identification problem from this MO point of view should be stated as:

$$\begin{array}{l}\min\limits_{\theta\in\mathbb{R}^6}\left[\frac{1}{N_{ailerons}}\sum\limits_{i=1}^{N_{ailerons}}\left(C_l(t_i) - \hat{C}_l(t_i,\theta)\right)^2,\right. \\ \left.\frac{1}{N_{rudder}}\sum\limits_{i=1}^{N_{rudder}}\left(C_l(t_i) - \hat{C}_l(t_i,\theta)\right)^2\right] \\ : \theta = \left[C_{l_0}, C_{l_\beta}, C_{l_p}, C_{l_r}, C_{l_{\delta_{al}}}, C_{l_{\delta_r}}\right]\end{array} \tag{36}$$

To solve the MOP stated above, any Multi-Objective optimizer can be used. In this work, the sp-MODE [1] algorithm has been chosen (Reynoso-Meza et al., 2010).

4. RESULTS

4.1 Flight Tests

In section 2.3 short maneuvers from a steady state flight are mentioned. In aeronautics, an airplane in steady flight is an aircraft which is maintaining constant heading and altitude, at a constant speed also and with leveled wings orientation (zero roll angle). At that point, the pilot does not need to make any correction on control surfaces or motor to maintain this steady flight.

In order to obtain data that can be employed in adjusting the aerodynamic parameters, the designed experiments simulate such short maneuvers. Thus, starting always at a steady state flight, each system input has been excited separately and, after that excitation, the aircraft has been left to evolve naturally, until the pilot deemed it appropriate and safe to recover the aircraft. Each experiment

[1] Available in http://www.mathworks.es/matlabcentral/fileexchange/39215-multi-objective-differential-evolution-algorithm-with-spherical-pruning

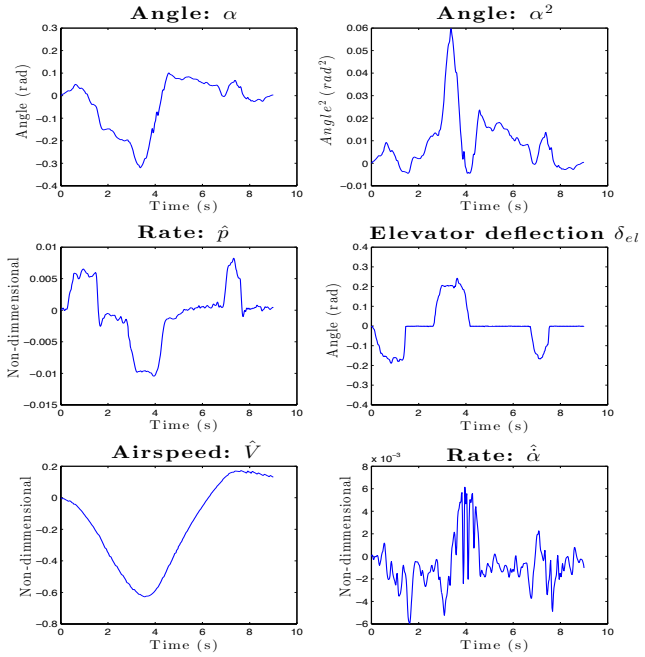

Fig. 2. Flight Test: longitudinal variables evolution in an elevators test

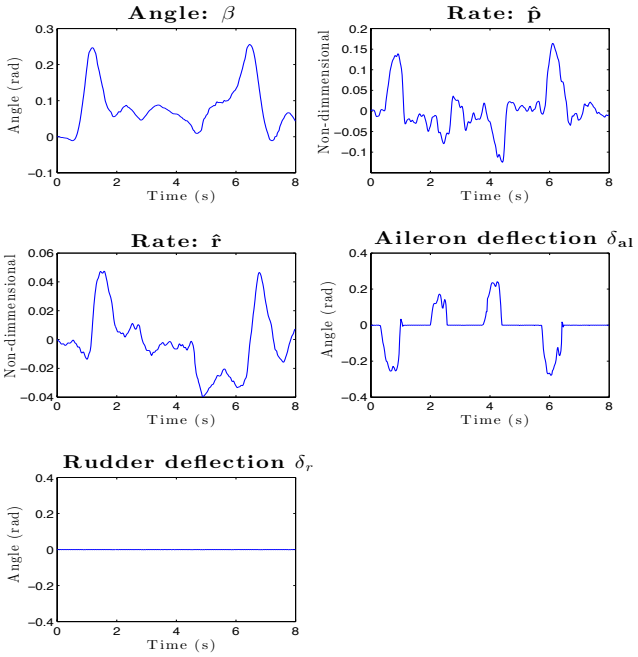

Fig. 3. Flight Test: lateral variables evolution in an ailerons test

has been performed twice, in order to count with different data sets for the adjustment and the validation. It should be noted finally, that in the absence of any sensor capable of measuring airspeed, all maneuvers described below have been carried out against the wind. This restriction was imposed to the pilot in order to reduce variability between tests.

The flight plan provided to the pilot before beginning the experiments was:

(1) Stable flight:
  (a) Adjust ailerons and rudder. Leveled wings.
  (b) Set the motor load around 50%.
  (c) Adjust elevators until the altitude gets constant without touching the control stick.
(2) Elevators up and down trying to copy a positive plus negative step sequence.
(3) Repeat step 1.
(4) Ailerons side to side in the appropriate frequency to avoid extreme rotations. First in one direction and then in the opposite one.
(5) Repeat step 1.
(6) Tail rudder side to side. First in one direction and then in the oposite one.
(7) Repeat step 1.
(8) Positive and negative steps in motor load. Sequence: 50%-100%-50%-0%-50%
(9) Repeat the whole process a second time.

Figures 2 and 3 show the evolution of the so called longitudinal and lateral variables during an elevators and ailerons excitation test respectively. As it can be seen, when a longitudinal input is excited, the rest of the longitudinal variables are excited too, which finally produces variations in the symmetrical aerodynamic coefficients. This same behaviour can be observed for the asymmetrical variables. All theese variations can be collected and used to calculate the aerodynamic derivatives of stability and control.

4.2 Optimization Results

Figure 4 shows the lateral models Pareto front found by the algorithm after the programmed optimization. As supposed, the better an experiment is fitted by a model, the greater error it gets for a second test. That is why the person in charge of identifying the aircraft model cannot be satisfied by using just one test, but should face the model to different experiments data.

Besides, confronting experiments in a multiobjective optimization, instead of using all of them as one in a monoobjective minimization, gives the main following advantages:

- Using multiobjective optimization involves the selection of a solution among others, which gives the designer the power of defining the importance of each experiment basing that definition on his requirements.
- The resultant Pareto front shows how good the different models are for each experiment. Thanks to that, the designer may get an idea of how good the collected data is and thereby, decide which are the requirements that he should ask for to the final model.
- It is possible to add as many objectives as wanted in the identification process. This means that confronting tests of the same kind is also possible, what could be a good practice for variability reducing.

For example, if the C_l coefficient is taken into account, it can be observed that the ailerons test gets a much better approximation than the rudder one. This fact, which can be deduced from the values that the square error takes, is also logical, since the ailerons are pricesely thought to introduce a moment in the X axis. In this case, the designer should probably prefer models which fit better this type of experiments over the ones that do a better job with rudder tests.

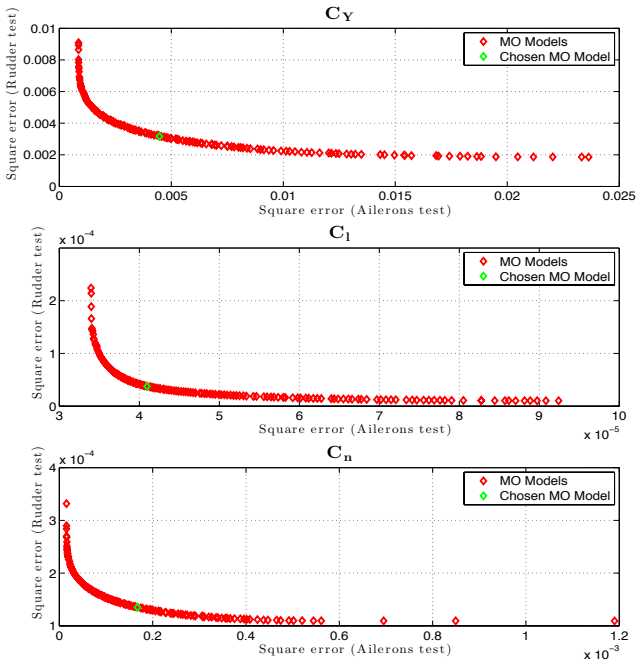

Fig. 4. Objetives space: Pareto Front of lateral models

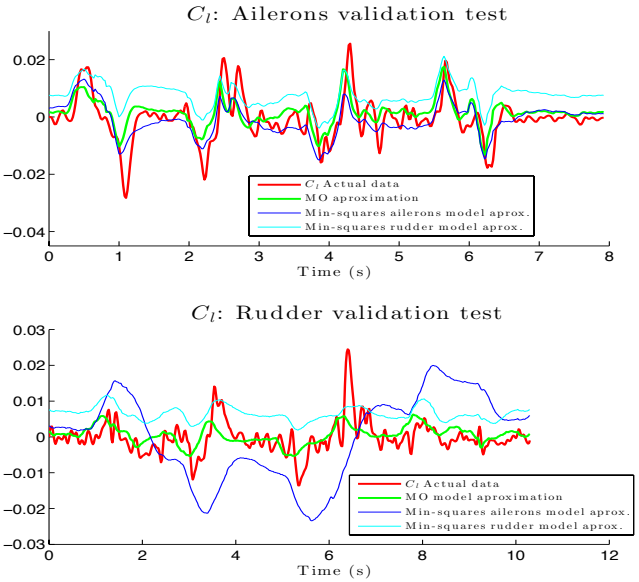

Fig. 5. C_l Validation results

The green point on figure 4 is the elected model for each of the lateral aerodynamic coefficients. It represents a solution of compromise between a situation in which the ailerons deflection is modified and a situation in which that modification is suffered by the tail rudder. This fact can be checked in figure 5. That graph shows the approximation to C_l (calculated with (30)) given by the chosen model for validation data. Two more models, identified by usig the classical least squares techinque, are also included in figure 5. Those two models represent the best approximation, in terms of MSE, for the ailerons and the elevators experiments separately (see Velasco (2013)). As can be deduced from the figure, the MO solution (green curve) represents a good intermediate approximation in both situations.

5. CONCLUSION

A methodolgy for the identification of UAVs aerodynamic models has been presented. Besides a demonstration of its application in a real system has been carried out with satistying results. The technique presented gives the already stated advantages in the data analysis and the identification process, since it involves a phase of decission by the designer. This phase allows then, the study of several models and the election of the one that fits better with the designer needs. In addition, confronting experiments offers information about the difficulties of finding a model that fits different flight conditions at the same time, which improves the understanding of the system. This technique may also give information about the importance of a particular kind of experiment in the identification of the model. All theese advantages lead to better models that may save time and money when designing autonomous aircraft control algotihms.

REFERENCES

Herrero, J., Blasco, X., Martínez, M., Ramos, C., and Sanchis, J. (2007). Non-linear robust identification of a greenhouse model using multi-objective evolutionary algorithms. *Biosystems Engineering*, 98(3), 335–346.

Klein, V. and Morelli, E.A. (2006). *Aircraft system identification: theory and practice*. American Institute of Aeronautics and Astronautics Reston, VA, USA.

Krüll, W., Tobera, R., Willms, I., Essen, H., and von Wahl, N. (2012). Early forest fire detection and verification using optical smoke, gas and microwave sensors. *Procedia Engineering*, 45, 584–594.

Reynoso-Meza, G., Sanchis, J., Blasco, X., and Martínez, M. (2010). Design of continuous controllers using a multiobjective differential evolution algorithm with spherical pruning. In *Applications of Evolutionary Computation*, volume 6024 of *Lecture Notes in Computer Science*, 532–541. Springer Berlin Heidelberg.

Rodriguez-Vazquez, K. and Fleming, P.J. (1998). Multi-objective genetic programming for nonlinear system identification. *Electronics Letters*, 34(9), 930–931.

Velasco, J. (2013). *Identificacion de modelos dinamicos y ajuste de controladores basado en algoritmos evolutivos multiobjetivo*. Master's thesis, Universidad Politécnica de Valéncia, Spain.

Velasco, J., García-Nieto, S., Reynoso-Meza, G., and Sanchis, J. (2013). Implementacion de un sistema hardware-in-the-loop para la simulacion en tiempo real de pilotos automaticos para UAVs. In *Actas de las XXXIV Jornadas de Automática*.

Velasco, J., García-Nieto Rodríguez, S., Reynoso Meza, G., and Sanchis Saez, J. (2012). Desarrollo y evaluación de una estación de control de tierra para vehículos aéreos no tripulados. In *Actas de las XXXIII Jornadas de Automática*.

Xiang, H. and Tian, L. (2011). Development of a low-cost agricultural remote sensing system based on an autonomous unmanned aerial vehicle (UAV). *Biosystems engineering*, 108(2), 174–190.

Yousefi, H., Handroos, H., and Soleymani, A. (2008). Application of differential evolution in system identification of a servo-hydraulic system with a flexible load. *Mechatronics*, 18(9), 513–528.